

Anomalous Wtb coupling effects in the weak radiative B -meson decay

Bohdan Grzadkowski and Mikołaj Misiak

*Institute of Theoretical Physics, University of Warsaw, PL-00-681 Warsaw, Poland
 and Theoretical Physics Division, CERN, CH-1211 Geneva 23, Switzerland*

(Received 25 February 2008; published 10 October 2008)

We study the effect of anomalous Wtb couplings on the $\bar{B} \rightarrow X_s \gamma$ branching ratio. The considered couplings are introduced as parts of gauge-invariant dimension-six operators that are built out of the standard model fields only. One-loop contributions from the charged-current vertices are assumed to be of the same order as the tree-level flavor-changing neutral current ones. Bounds on the corresponding Wilson coefficients are derived.

DOI: 10.1103/PhysRevD.78.077501

PACS numbers: 12.38.Bx, 13.20.He, 14.65.Ha

I. INTRODUCTION

The large $t\bar{t}$ production cross section at the LHC is expected to provide an opportunity to study Wtb interactions with high accuracy (see, e.g., [1,2]). When performing such studies, one should take into account constraints from the flavor-changing neutral current processes where loops involving top quarks play a crucial role. In particular, the inclusive decay $\bar{B} \rightarrow X_s \gamma$ provides stringent bounds on the structure of Wtb vertices.

In the present paper, we calculate contributions to the $\bar{B} \rightarrow X_s \gamma$ branching ratio from one-loop diagrams involving several dimension-six effective operators that give rise to nonstandard Wtb interactions. We work in the framework of an effective theory that is given by the Lagrangian

$$\mathcal{L} = \mathcal{L}_{\text{SM}} + \frac{1}{\Lambda} \sum_i C_i^{(5)} Q_i^{(5)} + \frac{1}{\Lambda^2} \sum_i C_i^{(6)} Q_i^{(6)} + \mathcal{O}\left(\frac{1}{\Lambda^3}\right), \quad (1)$$

where \mathcal{L}_{SM} is the standard model (SM) Lagrangian, while $Q_i^{(n)}$ denote dimension- n operators that are invariant under the SM gauge symmetries and are built out of the SM fields. Such an approach is appropriate for any SM extension where all the new particles are heavy ($M_{\text{new}} \sim \Lambda \gg m_i$). So long as only processes at momentum scales $\mu \ll \Lambda$ are considered, the heavy particles can be decoupled [3], which leads to the effective theory (1). Recent analyses of the top-quark anomalous couplings in the same framework can be found, e.g., in Refs. [4,5].

A complete classification of the operators $Q_i^{(5)}$ and $Q_i^{(6)}$ has been given in Ref. [6]. Since $Q_i^{(5)}$ involve no quark fields, we ignore them from now on, and skip the superscripts “(6)” at the dimension-six operators and their Wilson coefficients C_i . Here, we restrict our considerations to the following dimension-six operators that generate anomalous Wtb couplings:

$$\begin{aligned} Q_{RR} &= \bar{t}_R \gamma^\mu b_R (\tilde{\phi}^\dagger i D_\mu \phi) + \text{H.c.}, \\ Q_{LL} &= \bar{q}_L \tau^a \gamma^\mu q_L (\phi^\dagger \tau^a i D_\mu \phi) - \bar{q}_L \gamma^\mu q_L (\phi^\dagger i D_\mu \phi) \\ &\quad + \text{H.c.}, \\ Q_{LRi} &= \bar{q}_L \sigma^{\mu\nu} \tau^a t_R \tilde{\phi} W_{\mu\nu}^a + \text{H.c.}, \\ Q_{LRb} &= \bar{q}'_L \sigma^{\mu\nu} \tau^a b_R \phi W_{\mu\nu}^a + \text{H.c.}, \end{aligned} \quad (2)$$

where ϕ denotes the Higgs doublet, $\tilde{\phi} = i\tau^2 \phi^*$,

$$\begin{aligned} q_L &= (t_L, V_{tb} b_L + V_{ts} s_L + V_{td} d_L), \\ q'_L &= (V_{tb}^* t_L + V_{cb}^* c_L + V_{ub}^* u_L, b_L), \end{aligned} \quad (3)$$

and V stands for the Cabibbo-Kobayashi-Maskawa (CKM) matrix. The Wtb interaction vertex

$$\begin{aligned} \begin{array}{c} \uparrow \\ \text{q} \\ \text{t} \text{---} \text{b} \end{array} \text{---} W_\mu^a &= -\frac{ig_w}{\sqrt{2}} [\gamma_\mu (v_L P_L + v_R P_R) \\ &\quad + \frac{i\sigma_{\mu\nu} q^\nu}{M_W} (g_L P_L + g_R P_R)] \end{aligned} \quad (4)$$

with $P_{L,R} = \frac{1}{2}(1 \mp \gamma_5)$ is found by combining the usual SM interaction with the extra contributions that are obtained by setting the Higgs field in Eq. (2) to its vacuum expectation value.

Our operators (2) have been adjusted to generate the vertex (4) in a gauge-invariant manner, without introducing extra sources of CP -violation or tree-level flavor-changing neutral current (FCNC) interactions. The absence of tree-level FCNC in Q_{RR} , Q_{LRi} , and Q_{LRb} is transparent. Verifying that Q_{LL} is also free of tree-level FCNC requires a short calculation that is most conveniently performed in the unitary gauge when the pseudo-Goldstone components of ϕ are absent. The relative sign between the two parts of Q_{LL} causes cancellation of FCNC couplings like $\bar{s}_L \gamma_\mu b_L Z^\mu$. We wish to avoid such couplings here because they would contribute at the tree level to the observed decay $\bar{B} \rightarrow X_s l^+ l^-$.

Since our goal is testing anomalous couplings of the top quark without affecting topless physics, the flavor structure of Q_{RR} , Q_{LL} , and Q_{LRi} has been arranged in such a way that all the charged-current interactions in these operators involve the top. The operator Q_{LRb} does not fulfill this requirement. It contains some Wcb and Wub vertices, too. Using q_L instead of q'_L in this operator would cause problems with tree-level FCNC. Thus, our final $\bar{B} \rightarrow X_s \gamma$ results are going to receive contributions not only from the Wtb vertex (4) but also from the Wcb and Wub parts of Q_{LRb} , from the Wts and $\bar{t}t\gamma$ parts of Q_{LRi} (see Fig. 2 in the next section), as well as from the Wts part of Q_{LL} . The appearance of non- Wtb interactions is an unavoidable

consequence of introducing the anomalous Wtb ones in a gauge-invariant manner.

The dimensionless couplings $v_{L,R}$ and $g_{L,R}$ in Eq. (4) are related to the Wilson coefficients C_i as follows:

$$\begin{aligned} v_L &= V_{ib}^* + \frac{C_{LL} V_{ib}^*}{\sqrt{2} G_F \Lambda^2}, & v_R &= \frac{C_{RR}}{2\sqrt{2} G_F \Lambda^2}, \\ g_L &= \frac{C_{LRb} V_{ib}^*}{G_F \Lambda^2}, & g_R &= \frac{C_{LRt} V_{ib}^*}{G_F \Lambda^2}, \end{aligned} \quad (5)$$

where $G_F = 2^{-(5/2)} M_W^{-2} g_w^2$ is the Fermi constant. The coefficients C_i are real, which follows from the fact that the operators in Eq. (2) are self-conjugate. Note that all these operators become CP -even in the limit when the CKM matrix in Eq. (3) becomes real.

Constraints from $\mathcal{B}(\bar{B} \rightarrow X_s \gamma)$ on anomalous Wtb couplings have already been studied in Refs. [7,8]. However, those analyses were restricted to the couplings $v_{L,R}$ in Eq. (4). Moreover, our results for the branching ratio dependence on v_L are substantially different, because an operator containing the Wcb and Wub vertices was effectively used there instead of Q_{LL} .

II. MATCHING

In the decay $\bar{B} \rightarrow X_s \gamma$, all the external momenta are much smaller than M_W . Consequently, it is convenient to decouple the top-quark and the electroweak gauge bosons at the scale $\mu_0 \sim m_t, M_W$. At this scale, we match the effective theory (1) with another one, whose Lagrangian has precisely the same form as in the SM case [9]

$$\begin{aligned} \mathcal{L}_{\text{eff}} &= \mathcal{L}_{\text{QCD} \times \text{QED}}(u, d, s, c, b) \\ &+ \frac{4G_F}{\sqrt{2}} V_{ts}^* V_{tb} \sum_{i=1}^8 C_i(\mu) Q_i, \end{aligned} \quad (6)$$

where Q_1, \dots, Q_6 are four-quark operators, and

$$\begin{aligned} Q_7 &= \frac{em_b}{16\pi^2} \bar{s}_L \sigma^{\mu\nu} b_R F_{\mu\nu}, \\ Q_8 &= \frac{g_s m_b}{16\pi^2} \bar{s}_L \sigma^{\mu\nu} T^a b_R G_{\mu\nu}^a. \end{aligned} \quad (7)$$

The presence of non-SM terms in Eq. (1) causes deviations of $C_i(\mu_0)$ in Eq. (6) from their SM values

$$C_i(\mu_0) = C_i^{\text{SM}}(\mu_0) + \Delta C_i(\mu_0). \quad (8)$$

So long as $v_{L,R}$ and $g_{L,R}$ are treated as quantities of zeroth order in the expansion in g_w and g_s , the deviations $\Delta C_7(\mu_0)$ and $\Delta C_8(\mu_0)$ are also of zeroth order, similarly to $C_7^{\text{SM}}(\mu_0)$ and $C_8^{\text{SM}}(\mu_0)$. On the other hand, extra contributions to the Wilson coefficients of the four-quark operators Q_1, \dots, Q_6 arise only at higher orders in g_w or g_s , and will be neglected here.

Because of ultraviolet renormalization, it would be inconsistent to assume that no other operators but Q_{RR}, \dots, Q_{LRb} (2) are present in the dimension-six part of the Lagrangian (1). Instead, we shall make a weaker assumption, namely, that the $\overline{\text{MS}}$ -renormalized Wilson co-

efficients of all the other relevant operators in Eq. (1) at scales of order μ_0 satisfy

$$\frac{C_{\text{other}}(\mu \sim \mu_0)}{G_F \Lambda^2} \sim \mathcal{O}(g_w^n), \quad n \geq 2. \quad (9)$$

Under such an assumption, only tree-level $b \rightarrow s\gamma$ and $b \rightarrow sg$ diagrams with insertions of such operators must be included in our leading-order calculation of $\Delta C_7(\mu_0)$ and $\Delta C_8(\mu_0)$. Denoting such ‘‘primordial’’ tree-level contributions by $C_7^{(p)}(\mu_0)$ and $C_8^{(p)}(\mu_0)$, we can express $\Delta C_{7,8}(\mu_0)$ as follows

$$\begin{aligned} \Delta C_i(\mu_0) &= C_i^{(p)}(\mu_0) + \frac{1}{V_{ib}^*} \left[\delta v_L f_i^{v_L}(x) + v_R \frac{m_t}{m_b} f_i^{v_R}(x) \right. \\ &\quad \left. + g_L \frac{M_W}{m_b} f_i^{g_L}(x) + g_R \frac{m_t}{M_W} f_i^{g_R}(x) \right], \end{aligned} \quad (10)$$

where $x = m_t^2/M_W^2$ and $\delta v_L = v_L - V_{ib}^*$. It is understood that the Wilson coefficients in the definitions (5) of $v_{L,R}$ and $g_{L,R}$ are $\overline{\text{MS}}$ -renormalized at the matching scale μ_0 .

The functions $f_{7,8}^{v_{L,R}}(x)$ and $f_{7,8}^{g_{L,R}}(x)$ originate from ultraviolet-finite diagrams, and depend on x only. However, divergent diagrams occur in the calculation of $f_{7,8}^{g_{L,R}}(x)$. Consequently, logarithms $\ln \frac{\mu_0}{M_W}$ are present in these functions. They remain after applying the $\overline{\text{MS}}$ prescription for absorbing the divergences into the operators in Eq. (1) that generate $C_i^{(p)}(\mu_0)$. Several operators can serve as the corresponding counterterms—see section 4.8 of Ref. [6]. Our final results for $f_i^{g_{L,R}}(x)$ can be (and are) found without making any particular choice for the structure of these operators.

In Eq. (10) and everywhere in the following, nonlinear terms in $v_{L,R}$ and $g_{L,R}$ have been neglected. Including them in a consistent manner would require extending the operator basis (2) to operators of dimension higher than 6. Consequently, our calculation is valid only for $v_{L,R}, g_{L,R} \ll 1$, even though these quantities are formally treated as being zeroth order in g_w .

The functions $f_i^{v_L}(x)$ and $f_i^{v_R}(x)$ can be found without performing any new Feynman diagram computation. A brief inspection into the structure of Q_{LL} and Q_{RR} (most conveniently in the unitary gauge) reveals that all the relevant Feynman diagrams are identical to those that have already occurred either in the SM or in the LR -model [10] analyses of $b \rightarrow s\gamma$. Explicitly (see Eqs. (6) and (11) of Ref. [11] as well as Eqs. (3.2) and (4.6) of Ref. [10]):

$$\begin{aligned} f_7^{v_L}(x) &= \frac{3x^3 - 2x^2}{2(x-1)^4} \ln x + \frac{22x^3 - 153x^2 + 159x - 46}{36(x-1)^3}, \\ f_7^{v_R}(x) &= \frac{-3x^2 + 2x}{2(x-1)^3} \ln x + \frac{-5x^2 + 31x - 20}{12(x-1)^2}, \\ f_8^{v_L}(x) &= \frac{-3x^2}{2(x-1)^4} \ln x + \frac{5x^3 - 9x^2 + 30x - 8}{12(x-1)^3}, \\ f_8^{v_R}(x) &= \frac{3x}{2(x-1)^3} \ln x - \frac{x^2 + x + 4}{4(x-1)^2}. \end{aligned} \quad (11)$$

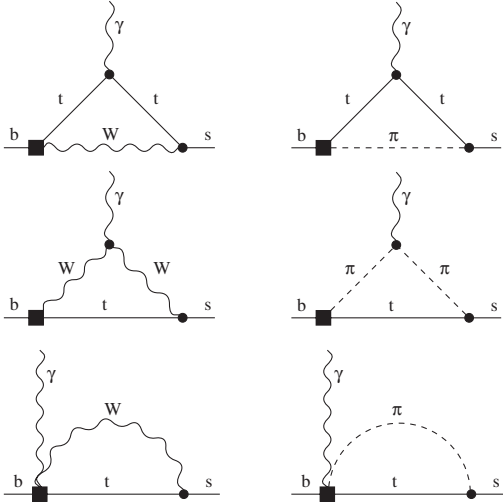


FIG. 1. Diagrams with non-SM $b \rightarrow t$ vertices that contribute to $f_7^{g_{L,R}}$. The pseudo-Goldstone boson is denoted by π .

As far as $f_7^{g_{L,R}}$ are concerned, our calculation of these functions has been performed in the Feynman-'t Hooft

$$\begin{aligned}
 f_7^{g_L}(x) &= \frac{x}{2} \ln \frac{\mu_0}{M_W} + \frac{-3x^4 + 26x^3 - 21x^2 + 4x}{12(x-1)^3} \ln x + \frac{3x^3 - 25x^2 + 16x}{12(x-1)^2}, \\
 f_7^{g_R}(x) &= -\frac{1}{4} \ln \frac{\mu_0}{M_W} + \frac{3x^4 - 12x^3 - 27x^2 + 32x - 8}{24(x-1)^4} \ln x + \frac{-15x^3 + 97x^2 - 69x + 11}{48(x-1)^3}, \\
 f_8^{g_L}(x) &= \frac{2x^3 - 6x^2 + x}{2(x-1)^3} \ln x + \frac{x^2 + 5x}{4(x-1)^2}, \\
 f_8^{g_R}(x) &= \frac{4x - 1}{2(x-1)^4} \ln x + \frac{2x^2 - 9x + 1}{4(x-1)^3}.
 \end{aligned} \tag{12}$$

The diagrams in Figs. 1 and 2 correspond to an off-shell calculation in the background-field gauge. Calculating on shell would bring some one-particle reducible diagrams into the game. Without the background field method, one would need to include additional diagrams with $W\gamma\pi$ couplings, where π stands for the pseudo-Goldstone boson. We have actually performed the calculation using both methods, which has served as a cross-check of the final result.

III. NUMERICAL RESULTS

Once the matching conditions are found, the calculation proceeds precisely as in the SM case. For the purpose of this section, we shall assume that $C_{7,8}^{(p)}(\mu_0)$ are real and neglect the imaginary part of V_{tb} . The $\bar{B} \rightarrow X_s \gamma$ branching ratio for arbitrary real values of $\Delta C_{7,8}(\mu_0)$ reads [12,13]

$$\begin{aligned}
 \mathcal{B} &\equiv \mathcal{B}(\bar{B} \rightarrow X_s \gamma)_{E_\gamma > 1.6 \text{ GeV}} \times 10^4 \\
 &= (3.15 \pm 0.23) - 8.0 \Delta C_7(\mu_0) - 1.9 \Delta C_8(\mu_0) \\
 &\quad + \mathcal{O}[(\Delta C_i)^2],
 \end{aligned} \tag{13}$$

for the numerical inputs as specified in Appendix A of Ref. [13], in particular, $\mu_0 = 160 \text{ GeV}$. Inserting our results from Eqs. (10)–(12) into Eq. (13), one finds

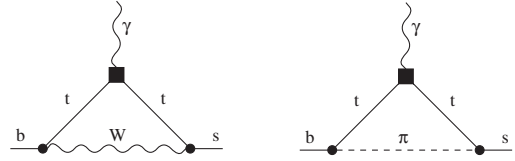


FIG. 2. Diagrams with non-SM $\bar{t}t\gamma$ vertices that contribute to $f_7^{g_R}(x)$.

gauge. The relevant Feynman diagrams with non-SM $b \rightarrow t$ vertices are shown in Fig. 1. In addition, analogous six diagrams with non-SM $t \rightarrow s$ vertices and two diagrams with non-SM $\bar{t}t\gamma$ vertices (Fig. 2) occur in the case of $f_7^{g_R}(x)$. In the case of $f_7^{g_L}(x)$, there are also diagrams where the intermediate t -quark gets replaced by u or c . The functions $f_8^{g_{L,R}}(x)$ have been found by replacing the external photon by the gluon in the diagrams like the ones in the first row of Fig. 1.

Our final results for $f_i^{g_{L,R}}(x)$ read:

$$\begin{aligned}
 \mathcal{B} &= (3.15 \pm 0.23) - 8.2 \delta v_L + 427 v_R - 712 g_L \\
 &\quad + 1.9 g_R - 8.0 C_7^{(p)}(\mu_0) - 1.9 C_8^{(p)}(\mu_0) \\
 &\quad + \mathcal{O}[(\delta v_L, v_R, g_L, g_R, C_i^{(p)})^2].
 \end{aligned} \tag{14}$$

As the reader might have expected, the coefficients at δv_L and g_R are of the same order as the first (SM) term, while the coefficients at v_R and g_L are substantially larger. For v_R and g_L , an enhancement [10,14] by m_t/m_b takes place, because the SM chiral suppression factor m_b/M_W gets replaced by the order-unity factor m_t/M_W . This was already evident in Eq. (10).

The negative coefficient at δv_L in Eq. (14) differs from the positive one in Fig. 1 of Ref. [8] where the leading-order (LO) expression for $C_7^{\text{SM}}(\mu_0)$ was used instead of our $f_7^{v_L}(x)$. The two quantities have different signs due to an additive constant in the relation

$$C_7^{\text{SM}}(\mu_0)_{\text{LO}} = \frac{1}{2} f_7^{v_L}(x) - \frac{23}{36}. \tag{15}$$

This constant originates from the SM loops where the top quark is replaced by the light ones (up and charm). No such loops are generated by our operator Q_{LL} . The flavor structure of the operators in Refs. [7,8] has not been specified in sufficient detail.

The appearance of $\ln\mu_0/M_W$ in Eq. (12) implies that the coefficients at g_L and g_R in Eq. (14) strongly depend on μ_0 . These coefficients are well approximated by $-379 - 485 \ln\mu_0/M_W$ and $-0.87 + 4.04 \ln\mu_0/M_W$, respectively. Their μ_0 -dependence and the one of $C_i^{(p)}(\mu_0)$ should compensate each other in Eq. (14), up to residual higher-order effects.

Taking into account the current world average [15]

$$\mathcal{B} = 3.55 \pm 0.24_{-0.10}^{+0.09} \pm 0.03, \quad (16)$$

one finds that a thin layer in the six-dimensional space $(\delta v_L, v_R, g_L, g_R, C_7^{(p)}(\mu_0), C_8^{(p)}(\mu_0))$ remains allowed by $b \rightarrow s\gamma$. When a single parameter at a time is varied around the origin (with the other ones turned off), quite narrow 95% C.L. bounds are obtained. They are listed in Table I. If several parameters are simultaneously turned on in a correlated manner, their magnitudes are, in principle, not bound by $b \rightarrow s\gamma$ alone. However, the larger they are, the tighter the necessary correlation is, becoming questionable at some point.

It is interesting to compare Table I with the sensitivity of top-quark decay observables to v_R, g_L and g_R . The ATLAS study in Ref. [1] reveals that their measurements should allow to put bounds on g_R at the level of (a few) $\times 10^{-2}$, i.e. stronger than the $\bar{B} \rightarrow X_s\gamma$ ones. On the other hand, the bounds they expect to set on v_R and g_L are more than an order of magnitude weaker than those in Table I, which is due to the previously mentioned m_t/m_b enhancement.

As far as δv_L is concerned, single top production measurements at the Tevatron imply $\delta v_L = 0.3 \pm 0.2$ [16]. Around an order of magnitude smaller uncertainty is expected at the LHC [17], which would definitely overcome the current $\bar{B} \rightarrow X_s\gamma$ bounds.

TABLE I. The current 95% C.L. bounds from Eq. (14) along the parameter axes for $\mu_0 = 160$ GeV.

| bound | δv_L | v_R | g_L | g_R | $C_7^{(p)}$ | $C_8^{(p)}$ |
|-------|--------------|---------|---------|-------|-------------|-------------|
| upper | 0.03 | 0.0025 | 0.0004 | 0.57 | 0.04 | 0.15 |
| lower | -0.13 | -0.0007 | -0.0015 | -0.15 | -0.14 | -0.56 |

IV. CONCLUSIONS

We have studied the effect of anomalous Wtb couplings on the $\bar{B} \rightarrow X_s\gamma$ branching ratio. The couplings were introduced via gauge-invariant dimension-six operators. Our results for the branching ratio dependence on g_L and g_R are new. In the case of δv_L , we have demonstrated the necessity of precisely defining the flavor structure of the relevant operators, which has not been previously done in sufficient detail.

The well-known m_t/m_b enhancement [10,14] implies that the $\bar{B} \rightarrow X_s\gamma$ bounds on v_R and g_L are much stronger than what one can possibly hope to obtain from studying the top-quark production and decay at the LHC. On the other hand, the future LHC bounds on δv_L and g_R are expected to overcome the current $\bar{B} \rightarrow X_s\gamma$ ones.

ACKNOWLEDGMENTS

We would like to thank G. Burdman, N. Castro, and M. Mangano for motivating remarks. This work has been supported in part by the Polish Ministry of Science and Higher Education as a research project N N202 006334 (in years 2008–11), by the EU-RTN Programme, Contract No. MRTN-CT-2006-035482, FLAVIANet, and by the Marie Curie Research Training Network HEPTOOLS, Contract No. MRTN-CT-2006-035505.

-
- [1] J. A. Aguilar-Saavedra, J. Carvalho, N. Castro, A. Onofre, and F. Veloso, *Eur. Phys. J. C* **53**, 689 (2008).
[2] M. M. Najafabadi, *J. High Energy Phys.* 03 (2008) 024.
[3] T. Appelquist and J. Carazzone, *Phys. Rev. D* **11**, 2856 (1975).
[4] P. J. Fox, Z. Ligeti, M. Papucci, G. Perez, and M. D. Schwartz, arXiv:0704.1482.
[5] Q. H. Cao, J. Wudka, and C. P. Yuan, *Phys. Lett. B* **658**, 50 (2007).
[6] W. Buchmüller and D. Wyler, *Nucl. Phys.* **B268**, 621 (1986).
[7] F. Larios, M. A. Perez, and C. P. Yuan, *Phys. Lett. B* **457**, 334 (1999).
[8] G. Burdman, M. C. Gonzalez-Garcia, and S. F. Novaes, *Phys. Rev. D* **61**, 114016 (2000).
[9] B. Grinstein, R. P. Springer, and M. B. Wise, *Phys. Lett. B* **202**, 138 (1988).
[10] P. L. Cho and M. Misiak, *Phys. Rev. D* **49**, 5894 (1994).
[11] C. Bobeth, M. Misiak, and J. Urban, *Nucl. Phys.* **B574**, 291 (2000).
[12] M. Misiak *et al.*, *Phys. Rev. Lett.* **98**, 022002 (2007).
[13] M. Misiak and M. Steinhauser, *Nucl. Phys.* **B764**, 62 (2007).
[14] K. Fujikawa and A. Yamada, *Phys. Rev. D* **49**, 5890 (1994).
[15] E. Barberio *et al.* (Heavy Flavor Averaging Group), arXiv:0704.3575.
[16] V. M. Abazov *et al.* (D0 Collaboration), *Phys. Rev. Lett.* **98**, 181802 (2007).
[17] D. O’Neil, B. Gonzalez-Pineiro, and M. Lefebvre, *J. Phys. G* **28**, 2657 (2002).